Photochemical interactions between pesticides and plant volatiles

Yara Arbid, Mohamad Sleiman, Claire Richard

Photochemical interactions between pesticides and plant volatiles

Yara Arbid, Mohamad Sleiman, Claire Richard*

Université Clermont Auvergne, CNRS, ICCF, F-63000 Clermont-ferrand, FRANCE

Abstract : Among the numerous studies devoted to the photodegradation of pesticides, very scarce are those investigating the effect of plant volatiles. Yet, pesticides can be in contact with plant volatiles after having been spread on crops or when they are transported in surface water, making interactions between the two kind of chemicals possible. The objectives of the present study were to investigate the reactions occuring on plants. We selected thyme as a plant because it is used in green roofs and two pesticides : the fungicide chlorothalonil for its very oxidant excited state and the insecticide imidacloprid for its ability to release the radical NO_2 under irradiation. Pesticides were irradiated with simulated solar light first in a solvent ensuring a high solubility of pesticides and plant volatiles, and then directly on thyme's leaves. Analyses were conducted by headspace gas chromatography-mass spectrometry (HS-GC-MS), GC-MS and liquid chromatography-high resolution mass spectrometry (LC-HRMS). In acetonitrile, chlorothalonil photosensitized the degradation of thymol, α-pinene, 3-carene and linalool with high quantum yields ranging from 0.35 to 0.04, and was photoreduced, while thymol underwent oxidation, chlorination and dimerization. On thyme's leave, chlorothalonil was photoreduced again and products arising from oxidation and dimerization of thymol were detected. Imidacloprid photooxidized and photonitrated thymol in acetonitrile, converting it into chemicals of particular concern. Some of these chemicals were also found when imidacloprid was irradiated dispersed on thyme's leaves. These results show that photochemical reactions between pesticides and the plants secondary metabolites

25 can take place in solution as on plants. These findings demonstrate the importance to increase
26 our knowledge on these complex scenarios that concern all the environmental compartments.
27 **Key-words** : Chlorothalonil, imidacloprid, thyme's leaves, photoreduction, photooxidation,
28 photonitration
29

Introduction

Pesticides undergo degradation processes in surface waters (Pehkonen and Zhang, 2002), on the surface of soil and of leaves (Katagi, 2004) yielding breakdown chemicals. The potential effects of these chemicals on wildlife and human health have attracted numerous studies aiming for identification and to improve knowledge on their physico-chemical, biological and toxicological properties (Martínez Vidal et al., 2019, de Souza et al., 2020).

Pesticides are generally photodegraded when they absorb solar light (Burrows et al., 2002, Mathon et al., 2021) or when they are irradiated in the presence of natural chromophoric species acting as sensitizers (natural organic matter) or photoinducers (nitrate ions, ferric species…) (Remucal, 2014, Ossola et al., 2021, Marussi and Vione, 2021, Brand et al., 1998). Photochemical reactions between two pesticides can also take place. In our group, we have demonstrated that mixing mesotrione and nicosulfuron (Ter Halle et al., 2010) or chlorothalonil and cycloxydim (Monadjemi et al., 2011) enhances the rate of photodegradation of each of them. Thiophanate-methyl was also shown to favor the photodegradation of methyl-bifenazate (Hamdache et al., 2018). These results were explained by the capacity of chlorothalonil and the primary photoproduct of thiophanate-methyl to generate oxidant triplet excited states and singlet oxygen capable of oxidizing other pesticides. In addition, reactions can be drastically affected by the medium. This was illustrated in the case of the insecticide methyl-bifenazate, the photodegradation of which was measured to be 70-fold faster on green pepper skin than on a film of paraffinic wax (Hamdache et al., 2018). This behaviour was rationalized by the presence of water from pepper. These results bring evidence that the fate of pesticides can be affected by the presence of other chemicals present in the medium apart from the well-known sensitizers or photoinducers.

Volatile compounds emitted by plants are the subject of intense research because of their implication in atmospheric chemistry, air pollution and defense of plants against pathogens (Atkinson and Arey 2003, Mellouki et al 2015, Wannaz et al, 2003, Hammerbacher et al, 2019). However, to the best of our knowledge, scenarios in which they could interact with pesticides were rarely considered in the literature. These potential reactions concern all the environmental compartments. When a pesticide is dispersed on the crop leaves just after been applied, it is surrounded by plant's volatiles facilitating reactions between each group of chemicals at the solid gas interface. Moreover, pesticides and plant volatiles can be transported to surface water after their solubilization in the run off water and can interact in the aquatic compartment. Plant volatiles correspond to a large group of chemicals : mono, di and triterpenes/terpenoids, phenols (Dudareva 2006, Abbas et al 2017, Mochizuki et al, 2020). They bear functionalities such as H-atoms, double bonds and aromatic rings giving them possibilities to be involved in a lot of photochemical reactions.

Here, we investigated the photochemical reactivity of two pesticides : the fungicide chlorothalonil (CT) and the insecticide imidacloprid (IMD) in the presence of the main thyme volatiles : thymol (T), linalool, 3-carene, α-pinene. These terpenes and thymol are common to other plant species (Carretero et al 2018). Both pesticides are susceptible to have an effect on the plant volatiles : CT shows photooxidant properties via its triplet excited state or the formation of singlet oxygen ($^1O_2$) (Ter Halle 2010) while IMD releases NO and NO_2 under irradiation making it a potential nitrosating/nitrating agent (Palma et al 2020). Out of nitrogen oxides, NO and NO_2 are considered toxic (Skalska et al., 2010). Experiments were first conducted in solution to evidence the reactions. Acetonitrile was chosen for its ability to ensure a high solubility of all the studied chemicals. Then, pesticides were directly irradiated on leaves of thyme to approach the real conditions closely.

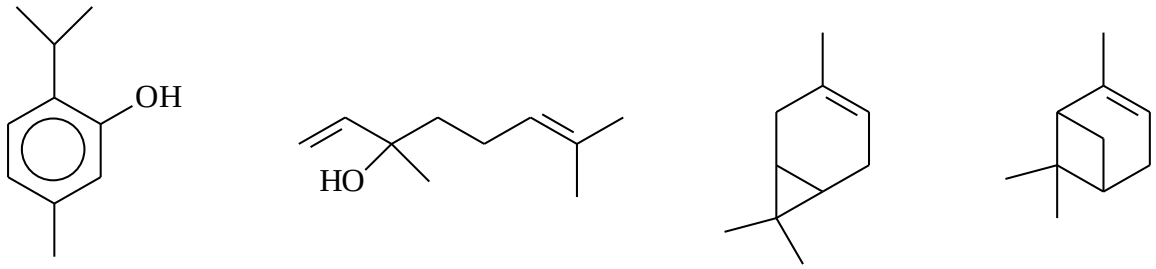

T Linalool 3-Carene α-Pinene

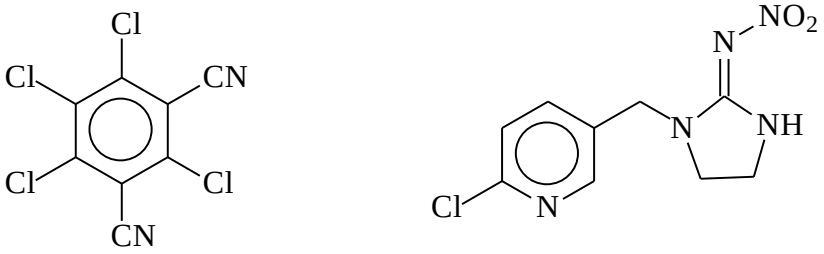

CT IMD

Scheme 1 : Structure of chlorothalonil (CT), imidacloprid (IMD), thymol (T), linalool, 3-carene and α-pinene

Experimental part

Chemicals and standards. IMD ($C_9H_{10}ClN_5O_2$) and CT ($C_8Cl_4N_2$) were purchased from Sigma Aldrich (Pestanal^{TM}, analytical standard, ≥ 98.0%). T ($C_{10}H_{14}O$, ≥ 98.5%), α-pinene ($C_{10}H_{16}$, 98%), 3-carene ($C_{10}H_{16}$, 90%), linalool ($C_{10}H_{18}O$, ≥ 97.0% GC area %), thymoquinone (TQ, $C_{10}H_{12}O_2$, ≥ 98%) were all purchased from Sigma Aldrich. Thymohydroquinone (TQH_2, $C_{10}H_{14}O_2$, 95%) was purchased from Enamine, Ukraine. All were used without further purification. Water was produced using a reverse osmosis RIOS 5 and Synergy (Millipore) device (resistivity 18 MΩ cm, DOC < 0.1 mg L^{-1}). Acetonitrile (ACN) was purchased from Carlo Erba Reagents (HPLC Plus Gradient grade-ACS-Reag). Thyme (*Thymus Vulgaris*) was freely grown under natural sunlight in a garden for seven years

in Beaumont (France) and regularly watered. In the case of IMD, we undertook a comparative set of experiments on a thyme plant (*Thymus Vulgaris*) bought in a garden center.

Samples preparation. All stock solutions were prepared in ACN and kept in the dark at 4°C before use. Final solutions were prepared by diluting stock solutions with ACN. For the experiments on thyme leaves, twigs were cut using scissors. Each twig contained 30 leaves (average area of each leave of 0.03 cm^2) for a total area of 1.8 cm^2 considering the two faces. Twigs were dipped in IMD or CT solution (7.5×10^{-4} M) for 30 s, left to dry freely for an hour, and then put in hermetically sealed headspace (HS) vials to be either used for control experiments in the dark or irradiated. Dark controls in the absence of pesticides were conducted with twigs directly put in HS vials. The surface concentration of IMD and CT on twigs was evaluated as follows : twigs covered by CT were immersed and agitated in 2 mL of acetonitrile for 2 min while those covered by IMD in 5 mL of acetonitrile. Solutions were then analyzed by high performance liquid chromatography coupled to a photodiode-array detector(HPLC-DAD) to determine the CT's and IMD's concentrations.

Irradiation. Solar UV radiations reaching the earth's surface contain UVA (315-400 nm) and a part of UVB (295-315 nm). The absorption spectrum of CT and IMD overlapping the radiations reaching the earth's surface within the wavelength range 295-350 nm (Figure SI-1A), we used the following irradiation devices to simulate solar light. The first one (device 1) was used to calculate the quantum yield of CT photodegradation in the presence of thyme's volatiles. Solutions containing CT (10^{-4} M) + volatiles (10^{-3} M) were put in a cuvette and irradiated at 313 nm (UVB) in parallel beam using a high pressure mercury lamp equipped with an Oriel monochromator. A radiometer QE65000 from Ocean optics was used to measure the photon flux I_0: $(3.0\pm0.2)\times10^{14}$ photons cm^{-2} s^{-1} at 313 nm. Samples were taken at chosen irradiation times and directly analyzed by HPLC-DAD to follow the degradation profile of CT. To monitor the disappearance of CT or IMD (10^{-4} M) in ACN alone or in the

presence of volatiles (10^{-3} M) and detect new photoproducts we needed to use a device delivering a more intense photon flux. Solutions (20 ml) were placed in a cylindrical Pyrex reactor (1.4 cm internal diameter) sealed with an air-tight silicon cap surrounded by 3 polychromatic tubes simulating UVB (Philips, TL20W/01-RS, λ_{max} = 313 nm) installed inside a custom-made cylindrical irradiation device (device 2). Aliquots were sampled at chosen irradiation times and directly analyzed by HPLC-DAD to monitor the degradation profiles of CT or IMD and UHPLC coupled to high resolution mass spectrometry (LC-HRMS) and gas chromatography coupled to mass spectrometry (GC-MS) to identify photoproducts. The third device (device 3) was a solar simulator CPS Atlas equipped with a xenon arc lamp, a filter cutting off wavelengths shorter than 290 nm and a cooling system maintaining the bottom of the device at 10°C. The global irradiance in the range of 300-800 nm was set at 500 W m^{-2}. It represents a medium value at 40°N latitude in summer. This device was used to irradiate the HS vials containing thyme twigs alone or covered with IMD or CT. In the case of IMD, 2 h of irradiation were enough to detect significant amounts of nitro derivatives of thymol. For CT, due to the difficulty to demonstrate the interaction between CT and thyme's volatile, we extended the irradiation until 6 h. Vials were then analyzed directly by Headspace gas chromatography coupled to mass spectrometry (HS-GC-MS) or chemicals contained in and on twigs were extracted by ACN as previously explained and analyzed by LC-HRMS or GC-MS. Irradiation experiments in solution were duplicated and on twigs duplicated or triplicated.

Analyses. UV-Vis absorption spectra of volatiles, CT, IMD, TQ, and TQH_2 were recorded using a Varian Cary 3 spectrophotometer. CT and IMD degradation profiles were tracked by HPLC-DAD using a NEXERA XR HPLC-DAD apparatus. The analytical column was a Phenomenex-kinetex C_{18} (100 mm×2.1 mm, 2.6 µm particle size) for CT experiments and EC 150/4.6 NUCLEODUR C_{18} endcapped column for IMD analyses. The eluent was a mixture of

147 ACN and water and the flow rate was set at 0.2 and 1 mL min^{-1} for CT and IMD,
148 respectively. The HPLC conditions for CT were as follows: the elution gradient started with
149 30% ACN maintained for 2 min and then linearly increased to reach 80% after 13 min; while
150 that for IMD started with 30% ACN which was maintained for 10 min. Photoproducts were
151 analyzed and quantified using HRMS on an Orbitrap Q-Exactive (Thermoscientific) coupled
152 to an ultra-high performance liquid chromatography (UHPLC) instrument Ultimate 3000
153 RSLC (Thermoscientific). The column was a Kinetec EVO C_{18} (100×2.1 mm), particle size of
154 1.7 µm (Phenomenex). The elution gradient started with 15% acetonitrile maintained for 5
155 min, then the percentage of acetonitrile was linearly increased to reach 55% after 5 min. The
156 flow was set at 0.45 mL min^{-1}. Analyses were made in positive (ESI^+/ESI^-) electrospray
157 mode. Identification of the major constituents was carried out using the Xcalibur software and
158 when necessary by matching retention times with those of authentic standards. The m/z of
159 proposed structures differed by less than 5 ppm from the theoretical mass. Standard solutions
160 of TQ were analyzed immediatly after have been prepared. The limit of detection LOD in the
161 case of TQ was estimated to 10^{-6} M by analyses of authentic solutions.
162 Photoproducts were also analyzed using an Agilent 6890 GC coupled to an Agilent 5973 MS.
163 The separation was carried out using a HP-5 µs column (25 m×0.25 mm×0.25 µm) operating
164 initially at 80°C over 1 min, followed by a 10°C min^{-1} ramp to reach 200°C and then a 30^0 C
165 min^{-1} ramp to reach 260°C maintained for 1 min (to calculate the degradation of terpenes) in
166 the case of CT experiments, while the analysis was operated initially at 70°C followed by a
167 10°C min^{-1} ramp to reach 160°C for 5 min and then a 30°C min^{-1} ramp to reach 250°C
168 maintained for 2 min in the case of IMD. The flow rate was 1 mL.min^{-1} with an injection
169 volume of 1 µL in both cases. T and some of its photoproducts were quantified after
170 derivatization with N,O-Bis (trimethylsilyl)trifluoroacetamide (BSTFA). The derivatizing

171 solution (2 mL) was prepared by mixing 60 µL of BSTFA with 1.4 mL sample. Separation
172 was achieved as previously described for CT experiments.
173 To determine the volatile metabolites produced by the plant, HS-GC-MS (Shimadzu HS-20
174 coupled with QP2010SE) was used. Twigs of 0.2 g alone or after dipping in CT solution were
175 transferred into a 20 mL headspace glass vial, then left in the dark or irradiated and incubated
176 for 5 min at 80^0 C. The analytical column (Mega 5-MS 30 m×0.25 mm) was operated
177 initially at 50°C for 1 min, followed by an 8°C min^{-1} ramp to reach 170°C and held for 4 min,
178 and then a 15°C min^{-1} ramp to reach 275°C maintained for 1 min. The mass spectrometer
179 source was heated to 200°C, and signals were detected between mass to charge ratios (m/z) of
180 50 and 350.
181 Identification of the major constituents was carried out using the NIST 17 database and when
182 necessary by matching retention times and ion fragments with those of authentic standards.
183 For calibration, a stock solution of T was prepared in ethanol at a concentration of 1 g L^{-1}.
184 Quantification of T was performed by means of 5-point calibration curve for which the
185 concentrations of standards ranged from 2-100 mg L^{-1}. All standard solutions were stored in
186 dark at 2-8°C in amber glass vials with Teflon-lined caps. They were found to be stable under
187 short-term (48 h) storage conditions. A linear response was obtained with a correlation
188 coefficient (R^2) of 0.997. Selectivity was evaluated by analyzing a set of blank samples and
189 monitoring the absence of interferences with S/N ratios higher than 3. No significant
190 interfering peaks were observed in the ion chromatogram time window monitored for T. The
191 precision of the method was determined by calculating the relative standard deviation (RSD)
192 of six replicate measurements of diluted T solution (10 mg L^{-1}). All RSDs were acceptable
193 and less than 7% indicating a good precision. The limit of detection LOD was calculated from
194 the standard deviation (σ) of multiple measurements (n=7) of diluted T solutions within a
195 factor of 5 of the background signal. LOD was set equal to 3σ which resulted in a value of 13

196 pg. The Limit of quantification (LOQ) was defined as 10σ or 43 pg. In all cases, LOD and
197 LOQ were significantly below the levels determined in the thyme extracts (0.07 to 2.7 mg).
198
199 **Quantum yields of CT photodegradation in the presence of terpenes in acetonitrile.** The
200 quantum yield of CT photodegradation (Φ_{CT}) was determined using **Eq 1**:
201 $\Phi_{CT} = \Delta c/(Ia \times \Delta t)$ **Eq 1**
202 where $\Delta c/\Delta t$ was the rate of CT consumption expressed in M s^{-1} and Ia was the rate of photon
203 absorption by CT at 313 nm expressed in Einstein L^{-1} s^{-1}. Ia was obtained using **Eq 2**:
204 $Ia = Io \times (1-10^{-\varepsilon \times \ell \times [CT]o}) \times 1000/\ell$ **Eq 2**
205 where $\varepsilon = 1760$ M^{-1} cm^{-1}, $[CT]_o = 10^{-4}$ M, and $\ell = 1$ cm.
206 **Laser flash photolysis.** Laser flash photolysis experiments were carried out using an Applied
207 Photophysics LKS.60 apparatus equipped with a Nd^{3+}:YAG laser Quanta-Ray GCR-130 used
208 in a right-angle geometry with respect to the monitoring light beam. Samples were irradiated
209 using the fourth harmonic (266 nm, 9 ns pulse duration) in a quartz cuvette. ^{3}CT* was
210 generated by irradiating CT (5×10^{-5} M in aerated ACN) and its decay monitored at 330 nm.
211 The reactivity of ^{3}CT* with thyme's volatiles was measured within the concentration range
212 10^{-4} - 2×10^{-3} M. In the case of IMD, no transient species were detected.
213 **Photoproducts toxicity**. The toxicity of photoproducts formed during the irradiations was
214 estimated using the freely available ECOSAR (ECOlogical Structure-Activity Relationship)
215 computer program (v 2.0). It predicts the toxicity of a molecule using a structure-activity
216 approach. The acute (LC50, the concentration that is lethal to half of fish after 96 h of
217 exposure to a certain molecule) and chronic toxicities (ChV) of CT, IMD, and formed
218 photoproducts on fish in fresh waters as well as logKow were obtained. The program (v 2.0)
219 is available from the website: epa.gov/tsca-screening-tools/ecological-structure-activity-
220 relationships-ecosar-predictive-model.

Results

1. Characterization of the thyme's constituents

This first objective was to determine what are the main volatile compounds in thyme's twigs, to estimate the amount of T in thyme's twig and to identify and quantify the chemicals related to T. Volatile compounds released from thyme's twigs after two hours in the dark in the HS vials were analyzed by HS-GC-MS (Figure SI-2). T, linalool, 3-carene and α-pinene were the main detected compounds. T is a phenolic compound while linalool, 3-carene and α-pinene are terpenes (Scheme 1). The amount of extractable T from thyme's twigs by ACN was measured by GC-MS. Based on several replicates using twigs containing 30 leaves (weight 0.2 g), it could be estimated to range between 0.35 and 2.7 mg per g of wet twigs. After that, we analyzed the non-volatile chemicals. For this, two vials containing two twigs each were left in the dark for 4h, extracted in 2 ml of ACN and analyzed by UHPLC-HR-MS and GC-MS. Several peaks directly connected to T were found (Table 1). By UHPLC-HR-MS, one got a peak at m/z = 165.0901 in ES^- corresponding to $[M+O-H^+]^-$ and named TO. By MS-MS, TO gave two main fragments at 149.0593 and 135.0443 corresponding to the loss of O and CH_2O, respectively (Figure SI-3). The oxidation of T can take place on the isopropyl group, on the methyl group or on the ring. No loss of H_2O was observed ruling out an oxidation of the isopropylic carbon atoms. The oxidation of the ring would lead to thymolhydroquinone. However, TO was not assigned to thymolhydroquinone because the two compounds had different retention times in HPLC (3.3 min for TO against 4.5 min for thymolhydroquinone), and different maximum of absorption (278 nm for TO against 290 nm for thymolhydroquinone). We therefore concluded that TO was the benzyl alcohol derivative (Table 1). The peak detected at m/z = 165.0901 in ES^+ (Figure SI-4) corresponded to [M+O-

$2H+H^+]^+$ and was assigned to the quinonic derivative TQ (Table 1). Its maximum of absorption at 250 nm was fully in line with this assignement. The other peak at m/z = 179.0704 in ES^- corresponding to $[M+2O-2H-H^+]^-$ was attributed to the quinonic derivative of TO, TQO (Figure SI-5). The two peaks showing m/z = 313.1806 and 329.1754 in ES^- were assigned to dimers, T-TO_{-2H} and TO-TO_{-2H}, respectively (Figures SI-6 and 7). By GC-MS, TO, TQ and several isomers of TO-TO_{-2H} were also detected.

The second objective was to investigate the effect of irradiation on the formation of these compounds. For this, two vials containing two twigs each were irradiated in the solar simulator for 4h and extracted using ACN. The same compounds were detected and the effect of irradiation on their formation can be seen in Table 2. The peak areas were between 15 and 100-fold higher after irradiation than in the dark showing the drastic effect of light.

2. Interactions between CT and thyme's volatiles

2.1. Irradiation of CT and thyme's volatiles in acetonitrile solution

Neither T, 3-carene, linalool and α-pinene nor CT underwent significant photodegradation when irradiated alone in ACN solution. Thyme's volatiles do not absorb the radiations emitted by the tubes (Figure SI-1B), while CT absorbs the radiations (Figure SI-1A) but yields a triplet excited state $^3CT^*$ efficiently deactivated by oxygen (7.8×10^8 M^{-1} s^{-1}, Monadjemi et al., 2011) (Figure 1A). In contrast, the irradiation of CT (10^{-4} M) in the presence of each of these volatiles (10^{-3} M) led to the fast disappearance of CT (Figure 1A) and the thyme's volatiles (Figure 1B). As shown in Figure 1A, the CT photodegradation increased in the order T > α-pinene > 3-carene > linalool. In accordance, the quantum yield of CT photodegradation (Φ_{CT}) was equal to 0.35, 0.20, 0.15, 0.04 for T, α-pinene, 3-carene and linalool, respectively against < 0.001 for CT alone. Concerning the thyme's volatiles loss, T was the fastest to disappear, followed by α-pinene, 3-carene, and linalool (Figure 1B).

To confirm the ability of thyme's volatiles to react with ^{3}CT* and measure the bimolecular rate constant of the reaction (k_r), we undertook laser flash photolysis experiments. CT was irradiated in the presence of each of these chemicals added at a concentration comprised between 3×10^{-4} and 2×10^{-3} M while the decay of ^{3}CT* was monitored at 330 nm (Figure 2). Alone, in air-saturated ACN, ^{3}CT* disappeared by an apparent first order kinetic with $k = 1.6\times10^6$ s^{-1} corresponding to the sum $k_d + k_{O2}[O_2]$, where k_d is the rate constant of deactivation by collision with the solvent molecules, k_{O2} the rate constant of reaction with oxygen and $[O_2]$ the concentration of oxygen in the solution. In the presence of T, ^{3}CT* disappeared faster than alone showing that a reaction between ^{3}CT* and T took place (Figure 2A). This reaction might be an energy transfer or an electron/H atom transfer reaction. The energy level of ^{3}CT* was previously estimated to lay at 275 kJ mol^{-1} based on phosphorescence measurements at 77 K in pentane (Porras et al, 2014). This is lower than the energy level reported for phenol ~ 314-334 $kJ.mol^{-1}$ (Becker, 1969) making the energy transfer from ^{3}CT* to T unlikely. Moreover, given the ability of ^{3}CT* to oxidize phenols (Monadjemi et al., 2011), an electron or H atom transfer from T to ^{3}CT* with formation of the reduced CT radical ($CT^{\cdot-}/CTH^{\cdot}$) and the phenoxyl radical ($T_{-H}^{\cdot}$) (Scheme 2) looks more probable .

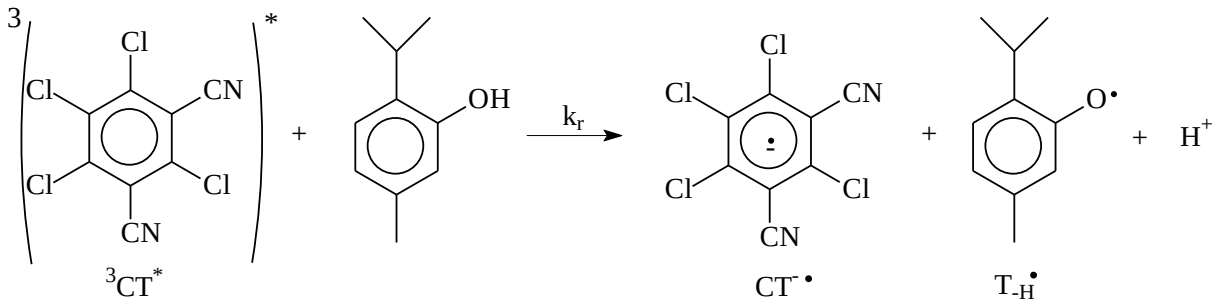

Scheme 2 : Reaction of ^{3}CT* with thymol

The shape of the time-resolved absorption spectrum of Figure 3A revealed the formation of a secondary species that could be therefore either the reduced CT radical or $T_{-H}^{\cdot}$. Its significant absorption measured at 330 nm matches more with the reduced CT radical (Bouchama et al., 2014) than with $T_{-H}^{\cdot}$ that shows maxima at 390 and 410 nm (Venu at al., 2013). Due to the overlapping of the two species absorption, a numerical analysis of the differential equations was necessary to determine the k_r value. The best fit of the experimental data was obtained by taking $k_r = 7.0\times10^9$ M^{-1} s^{-1}, $\varepsilon_{CT*}/\varepsilon_{phenoxyl} = 2.0$, and a first order decay rate constant of 5×10^5 s^{-1} for the reduced CT radical in air-saturated medium (Monadjemi et al., 2014). Individual evolution of these species are shown in the inset of Figure 2A.

In the case of α-pinene, 3-carene and linalool, the absorbance at 330 nm completely decayed within 1 μs following the flash (Figure 2B). This result demonstrated the reaction of ^{3}CT* with terpenes. However, with these compounds, the formation of the reduced CT radical was not observed (Figure 2B). Values of k_r could be deduced from the linear plot of k, the obserbed first order rate constant, vs [terpene] (inset of Figure 2B). Assuming $k = k_d + k_{O2}[O_2] + k_r[terpene]$, one got $k_r = 2.6\times10^9$, 2.8×10^9 and 3.9×10^9 M^{-1} s^{-1} for α-pinene, 3-carene, and linalool, respectively. The oxidation of terpenes by ^{3}CT* was likely due to the

presence of labile H atoms in their structures and the non-observation of the 330 nm radical could be tentatively explained by an in-cage reaction between the reduced CT radical and the oxidized terpene radical leading directly to photoproducts (Scheme 3 in the case of 3-carene). If one admits that the relative importance of process *a* that yielded photoproducts and process *b* in which CT was regenerated depended on the structure of the terpene, then one can also explain why Φ_{CT} varied from 0.20 for α-pinene to 0.04 for linalool whereas the k_r values laid in a very narrow range for these two compounds. Finally, we found that all four thyme's volatiles readily reacted with ^{3}CT*. The higher reactivity of T compared to that of α-pinene, 3-carene, and linalool is in line with the presence of an easily abstractable phenolic H atom.

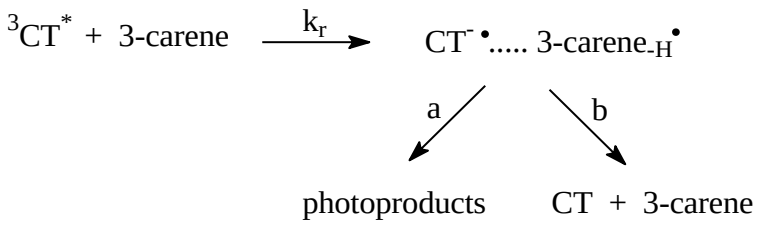

Scheme 3 : Reaction of ^{3}CT* with 3-carene

Product studies was also undertaken by GC-MS and UHPLC-HRMS . For the CT+T mixture, we detected a new photoproduct showing m/z = 183.0571 and 185.0542 in ES^- along with TO, TQ, TQO, T-TO_{-2H} and TO-TO_{-2H}. This compound corresponded to $[T\text{-}H+Cl\text{-}H^+]^-$ and was named TCl (Table 1). By GC-MS, we detected TCl again, CT_{-Cl} and CT_{-2Cl}. The formation of dechlorinated CT confirmed that photoreduction took place. CT_{-Cl} was also detected upon the irradiation of CT+3-carene, but no other photoproducts were found by GC-MS and no photoproducts at all were detected with α-pinene and linalool.

Based on these data and on the known CT photoreactivity, the reaction pathways shown in Scheme 4 can be proposed to explain the reaction between CT and T. In neat acetonitrile, ^{3}CT* is generated with a quantum yield close to unity and trapped by O_2 (k_{O2} = $(1\pm0.1)\times10^9$ M^{-1} s^{-1}) to yield $^1O_2$ with a quantum yield equal to 0.85±0.06 (Bouchama et al, 2014). T will therefore compete with O_2 for the reaction with ^{3}CT*. Taking $k_r = 7.0\times10^9$ M^{-1} s^{-1} and $[O_2] = 1.9\times10^{-3}$ M in air-saturated acetonitrile solution at 24°C (Murov et al, 1993), one can estimate that T (10^{-3} M) could trap 79% of ^{3}CT* while 21% of O_2. In our experimental conditions, T was thus mainly photooxidized through a direct reaction with ^{3}CT*, however, given the known good reactivity of singlet oxygen with phenolic compounds (Wilkinson and Brummer, 1981), a part of the loss of T may be attributable to the reaction T + $^1O_2$. Once formed, $T_{-H}^{\cdot}$ should be further oxidized into TO, TQ and yield dimeric species. The detection of TCl demonstrates that CT can also photoinduce the chlorination of other chemicals. A possible explanation is the release of chlorine atoms from $CT^{-\cdot}$ followed by their recombination with $T_{-H}^{\cdot}$ (Scheme 4). Such a reaction also rationalizes the formation of dechlorinated CT.

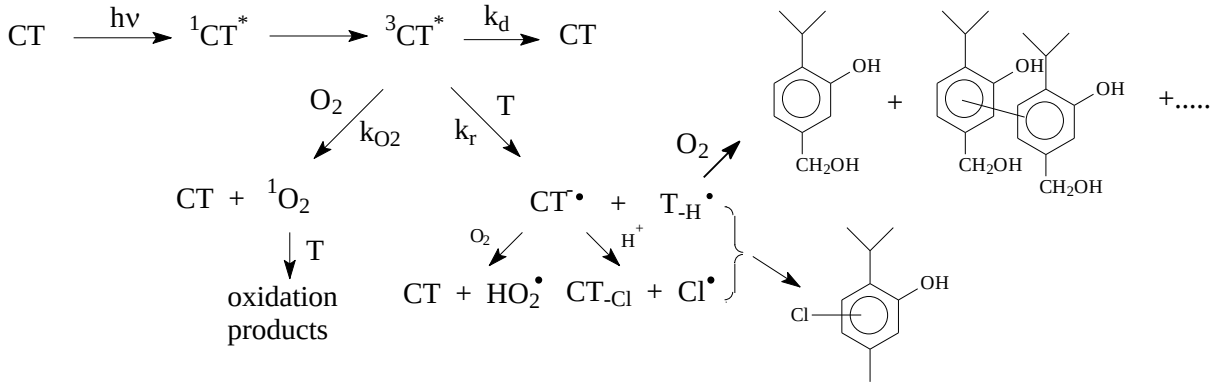

Scheme 4: Mechanism of CT photolysis in the presence of T

The values of k_r for terpenes were 1.8 to 2.7-fold lower than for T. Therefore, the percentage of ^{3}CT* trapped by terpenes at 10^{-3} M should be consequently lower than for T and the amount of singlet oxygen generated higher. The photooxygenation of terpenes bearing double bonds such as α-pinene, linalool and 3-carene is therefore likely in our conditions, given their reactivity with singlet oxygen (Chiron et al, 1997).

Similar reactions can take place in water or in media enriched in water because ^{3}CT* was also detected in water/acetonitrile (90 :10, v/v) with a quantum yield of formation also close to unity (Bouchama et al, 2014). However, changing the solvent is expected to induce some changes in the pathway ratios. For instance, the percentage of ^{3}CT* trapped by O_2 will decrease significantly from acetonitrile to water because the O_2 concentration is reduced by a factor of about 7 (from 1.9×10^{-3} M to 2.7×10^{-4} M in air-saturated solutions at 24°C). This may favor the direct reaction between ^{3}CT* and the two volatiles T and linalool for which the water solubility is good and thus the CT photoreduction. In contrast, for 3-carene and α-pinene that show a very low water solubility, CT photoreduction should be insignificant and ^{3}CT* could mainly lead to singlet oxygen. However, the lifetime of singlet oxygen is shorter in water (4 μs, Rodgers and Snowden, 1982) than in acetonitrile (61-68 μs, Hurst et al., 1982) which will affect negatively the rate of terpenes photooxidation. Last, the higher polarity of water compared to acetonitrile may increase k_r, although it is already quite high in acetonitrile.

2.2. Irradiation of CT on thyme's leaves

We started the experiments on thyme's leaves by estimating the amount of CT deposited on two twigs after their dipping in a solution of CT (7.5×10^{-4} M). In the 2 ml of ACN used for the extraction, the CT concentration was of 3.4×10^{-5} M. Based on a total leaves

376 area of 3.6 cm^2, we finally got a CT concentration of 5±1 μg per cm^2, which is in the range of
377 the surfacic concentrations calculated for typical CT application rates of 0.5-1 kg ha^{-1}.

378 Then, CT was irradiated for 6 h in the solar simulator on thyme's leaves or deposited
379 on a glass dish chosen as an inert support and ACN extracts analysed by GC-MS (Figure 4).
380 While no CT photodegradation was observed on dishes, an almost full loss of CT on thyme's
381 leaves was measured. CT_{-Cl} and CT_{-2Cl} were formed (Inset of Figure 3) confirming the
382 photoreduction of CT when applied on thyme's leaves. T that was present in high amounts in
383 the thyme's twigs was the candidate to induce this photoreduction, even though its
384 involvement in the reaction cannot firmly demonstrated.

385 Moreover, the GC-MS area of T peak increased similarly after 4 h of irradiation for
386 thyme's twigs irradiated in the absence of CT and for thyme's twigs irradiated in the presence
387 of CT from $(2.8\pm0.4)\times10^6$ to $(2.3\pm0.9)\times10^8$ (Table 2). The presence of CT did not affect the
388 nature of T byproducts (TO, TQ, TQO, $T\text{-}TO_{-2H}$ and $T\text{-}TO_{-2H}$) and their peak area measured
389 after 4 h of irradiation and in the dark (Table 2). The only evidence of an interaction between
390 CT and T came from the analyses of the gazeous phase of irradiated vials by HS-GC-MS.
391 Indeed, in this case, a drastic loss of T was observed (Figure SI-8). The apparent discrepancy
392 between the HS-GC-MS analyses conducted directly on the volatiles present in the vials and
393 the GC-MS analyses that required extraction of chemicals by ACN can be explained as
394 follows. CT deposited on leaves consumed T present in the gazeous phase, and the weak
395 volatility of T limited any reequilibration through remission from leaves allowing to detect the
396 T loss by HS-GC-MS. However, this T consumption was not measurable after extraction by
397 ACN because extraction allowed the recovering of the great part of T present in the leaves
398 while the loss of T that was related to the initial concentration of CT on the twigs laid below
399 the measurement uncertaincies. Indeed, we estimated that 5.7×10^{-7} mole of T could be
400 extracted while 6.7×10^{-8} mole of CT were present on twigs. As one mole of CT was expected

401 to oxidize one mole of T at its best, the amount of T consumed was less than 12% of T
402 extracted, thus negligible.

403 To conclude, we demonstrated that in solution photochemical reactions between CT
404 and thyme's volatiles, in particular T, took place with photoreduction of CT and
405 photooxidation/photochloration of T. On thyme's leaves, photoreduction of CT was also
406 observed. The involvement of T in this reaction was likely based on the data obtained in
407 solution, but could not be firmly confirmed.

408

409 **3. Interactions between IMD and thyme's volatiles**

410 **3.1. Irradiation of IMD and T in acetonitrile solution**

411 After 30 min of irradiation alone in device 2, IMD (10^{-4} M) disappeared by 6.5×10^{-5} M
412 (65%). Three photoproducts were identified (Table 3). The main one gave a peak at m/z =
413 211.0742/213.0710 in ES^+ (Figure SI-9) and corresponded to $[M\text{-}NO_2+H+H^+]^+$, it was
414 assigned to the imino derivative $IMD_{\text{-NO2+H}}$. Two other minor peaks were detected at m/z =
415 223.0385/225.0356 in ES^- (Figure SI-10) corresponding to $[M\text{-}NO\text{-}H\text{-}H^+]^-$ and at m/z =
416 432.0744/434.0715/436.0689 (Figure SI-11) corresponding to $[2M\text{-}N_2O_3\text{-}H^+]^-$. They were
417 named $IMD_{\text{-HNO}}$ and $IMD\text{-}IMD_{\text{-N2O3}}$, respectively.

418 In the presence of T (10^{-3} M), IMD disappeared by 3.0×10^{-5} M (30%) after 30 min of
419 irradiation (Table 4), i. e. less than alone. On the other hand, the T loss was of 7% after 2 h,
420 yielding a consistent consumption of around 1.7×10^{-5} M after 30 min (Table 4). $IMD_{\text{-NO2+H}}$,
421 $IMD_{\text{-HNO}}$ and $IMD\text{-}IMD_{\text{-N2O3}}$ were detected again but in much smaller amounts than in the
422 absence of T (Table 4). In addition, we detected along TO, a peak at m/z = 194.0812 in ES^-
423 (Figure SI-12) corresponding to $[M+NO_2\text{-}H\text{-}H^+]^-$ and assigned to nitrothymol TNO_2, a second
424 peak at m/z = 210.0761 in ES^- (Figure SI-13) corresponding to $[M+O+NO_2\text{-}H\text{-}H^+]^-$ assigned to
425 nitrated TO, as well as traces of a peak at m/z = 358.1649 in ES^- corresponding to the dimer

426 [2M+O+NO_2-H-2H-H^+]$^-$ and labelled TO-TNO_2. Although solutions were carefully handled
427 in the dark, traces of TNO_2 were detected in the non-irradiated solutions. It seemed therefore
428 that IMD was also able to release some NO_2 molecules, spontaneously.

429 These results showed that T inhibited the IMD photodegradation and the
430 photoproducts formation, in particular that of IMD_{-HNO} and IMD-IMD_{-N2O3} while undergoing
431 nitration. This inhibition strongly suggests that competition between T and IMD took place.

432

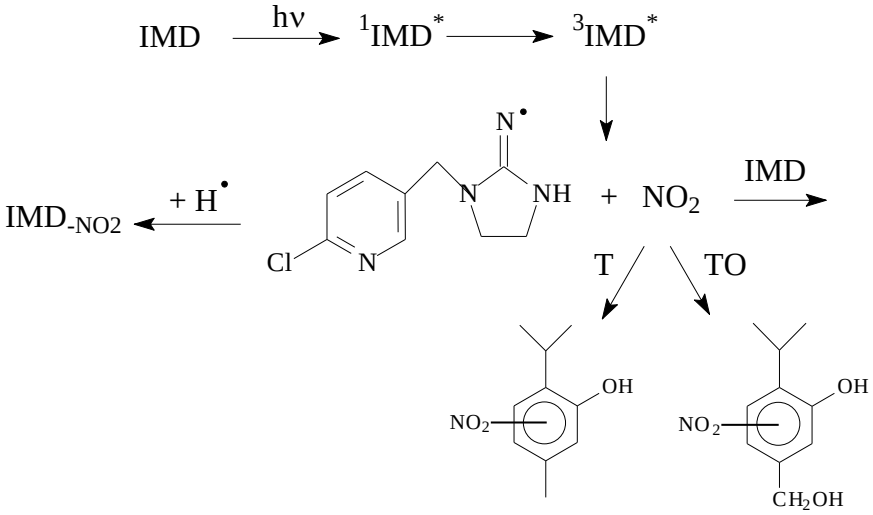

433

434 Scheme 5 : Mechanism of IMD photolysis in the presence of T

435

436 As shown in scheme 5, the excitation of IMD released NO_2 by the cleavage of the N-
437 NO_2 bond and led to the formation of the radical IMD_{-NO2} that is further converted into IMD_{-NO2+H} after the abstraction of an H atom (Palma et al., 2020). The formation of TNO_2 could be
439 explained by the oxidation of T by NO_2 into the corresponding phenoxyl radical followed by
440 the addition of NO_2 onto it (Marussi and Vione, 2021). Similarly, the nitration of TO into
441 $TONO_2$ should involve the oxidation of TO by NO_2 followed by the addition of NO_2 on the
442 corresponding phenoxyl radical. The lower rate of IMD loss in the presence of T was in favor

443 of a competition between IMD and T for the reaction with NO_2 and suggests that NO_2 reacted
444 with IMD, for example, by H atom abstraction.
445
446 **3.2. Irradiation of IMD on thyme's leaves**
447 As for CT, we estimated the amount of IMD deposited on two twigs after their dipping
448 in a solution of IMD (7.5×10^{-4} M). In the 5 ml of ACN used for the extraction, we measured a
449 IMD concentration of 3.9×10^{-5} M. Based on a total leaves area of 3.6 cm^2, we finally got a
450 IMD concentration of 14±2 μg per cm^2 that is enough to observe reactions.
451 Vials containing twigs covered with IMD were irradiated in the solar simulator for 2 h,
452 and in parallel other vials were left in the dark for the control. The ACN extracts were then
453 analyzed by UHPLC-HR-MS. In the samples left in the dark, we detected TO, TNO_2, $TONO_2$
454 and TO-TNO_2 (Table 4), confirming that the NO_2 release from IMD could also take place in
455 the dark. As shown in Table 4, upon irradiation of IMD on twigs, TNO_2 and TO-TNO_2 where
456 detected in amounts equivalent to those observed in the dark . However, for $TONO_2$ a 50-
457 folds enhancement was measured. The presence of IMD little increased the formation of TO
458 compared to thyme irradiated in the absence of IMD. Another set of experiments was
459 undertaken on the same variant of thyme just bought in a garden center and thus much
460 younger and much less exposed to solar light. In this case also, nitration reactions were
461 observed under irradiation but they yielded TNO_2 and not $TONO_2$ as for the older thyme.
462 Accordingly, the young thyme contained much less TO than the older one.
463 Therefore, we conclude that IMD generated nitrocompounds when it was in contact
464 with T, with an increase of the phenomenon under light exposure. The reaction involved the
465 radical NO_2 that was released in the medium mainly photochemically but also spontaneously.
466 T had also an effect of the fate of IMD : by quenching NO_2, it increased its lifetime.
467

4. Estimation of the photoproducts toxicities

Using the ECOSAR computer program (version 2.0), we estimated the potential acute (LC_{50}) and chronic toxicity (ChV) of the starting chemicals and their degradation products (Table 5). CT is classified as a moderate toxic chemical. Its photoreduction by T and terpenes in CT_{-Cl} and CT_{-2Cl} decreases the acute and chronic toxicity on fish from 6.98 to 74.40 mg L^{-1} and 0.81 to 7.57 mg L^{-1}, respectively and also the bioaccumulation, but these compounds are still classified as moderatly toxic compounds. On the other hand, TO is less toxic on fish than T with LC_{50} of 20.90 against 1.86 mg L^{-1} and ChV of 2.08 against 0.21 mg L^{-1} and less bioaccumulated. In contrast, TQ, $T\text{-}TO_{-2H}$, $TO\text{-}TO_{-2H}$ and TCl are more toxic than T with $LC_{50} \leq 1.12$ mg L^{-1} and ChV ≤ 0.16. TQ, $T\text{-}TO_{-2H}$ and TCl are classified as highly toxic. TCl was not detected in the experiments on thyme's leaves, this might be due to a high value of K_{ow} and a diffusion of this compounds inside the cuticle preventing its extraction by ACN. In the case of IMD, T inhibited the pesticide degradation rate and any new chemical deriving from IMD was formed. Other good H-donor chemicals such as phenolic compounds contained in plants may have the same effect and therefore increase the lifetime of IMD and lengthen its insecticidal effect. T and TO underwent nitration. $TONO_2$ is moderatly toxic as T with higher LC_{50} but lower ChV, while TNO_2 is classified as highly toxic with LC_{50} = 1.39 mg L^{-1} and CHV = 0.15. Therefore, chemicals that are more toxic than the starting compound can be formed during these reactions.

Conclusion :

In this work, we investigated the photochemical reactions between pesticides and plant's volatiles in solution and leaf surfaces and we demonstrated that interactions take place

in both media. The interactions modified the fate and the transformation pathways of the chemicals and depended on the chemicals structure and the matrix. This was illustrated by the examples of the fungicide chlorothalonil and the insecticide imidacloprid chosen as pesticides and thymol, α-pinene, 3-carene and linalool as plant's volatiles. Studying these reactions is relevant for several reasons. First, they can occur in the real conditions on plants and in surface waters and affecting the fate of the chemicals, these reactions can also alter the phytosanitary treatments shortening the lifetime of the pesticide for example, and lead to repeated and/or increased treatments. These are therefore important factors to consider in the design of pesticides. Secondly, the interactions can potentially generate toxic by-products leading to the pollution of water bodies and of air. The air pollution may be observed in particular in the cities where green roofs are installed. Indeed, their growth in many urban zones in the world could be accompagnied by increased possibilities of reactions between plant's volatiles and other chemicals such as the pesticides used to protect the roof plants which might finally lead to an enhanced formation of by-products. For all these reasons, it seems necessary to get a better insight into these overlooked reactions often referred to as « cocktail effect ».

Acknowledgments :

This research was supported by a PhD fellowship from the University Clemront-Auvergne/French Ministry of Higher Education and Research. The authors would like to thank Martin Leremboure (Engineer CNRS) and Frédéric Emmenegger (Tech CNRS) for UHPLC-MS analyses, and Guillaume Voyard (Engineer CNRS) for HPLC-DAD analyses.

References

F. Abbas, Y. Ke, R. Yu, Y. Yue, S. Amanullah. Volatile terpenoids: multiple functions, biosynthesis, modulation and manipulation by genetic engineering. Planta (2017) 246, 803–816.
doi.org/10.1007/s00425-017-2749-x

R. Atkinson, J. Arey. Atmospheric Degradation of Volatile Organic Compounds. Chem. Rev. (2003) 103, 12, 4605–4638
doi.org/10.1021/cr0206420

R. S. Becker « Theoritical and Interpretation of fluorescence and phosphorescence » Wiley-Interscience, New-York, 1969.

S. Bouchama, P. de Sainte-Claire, E. Arzoumanian, E. Oliveros, A. Boulkamh, C. Richard Photoreactivity of chlorothalonil in aqueous solution. Environ Sci Process Impacts (2014) 16(4) 839-847
doi.org/10.1039/C3EM00537B

N. Brand, G. Mailhot, M. Bolte
Degradation Photoinduced by Fe(III): Method of Alkylphenol Ethoxylates Removal in Water. Environ. Sci. Technol. (1998) 32, 2715–2720
doi.org/10.1021/es980034v

H.D. Burrows, M. Canle L, J.A. Santaballa, S. Steenken. Reaction pathways and mechanisms of photodegradation of pesticides. J. Photochem. Photobiol. B (2002) 67, 71-108
doi.org/10.1016/S1011-1344(02)00277-4

F. Chiron, J.C. Chalchat, R.P. Garry, J.F. Pilichowski, J. Lacoste. Photochemical hydroperoxidation of terpenes I. Synthesis and characterization of α-pinene, β-pinene and limonene hydroperoxides. J. Photochem. Photobiol. A: Chemistry (1997) 111, 75-86. doi.org/10.1016/S1010-6030(97)00184-6

N. Dudareva , F. Negre , D. A. Nagegowda, I. Orlova. Plant Volatiles: Recent Advances and Future Perspectives. Crit Rev Plant Sci (2006) 25, 417-440 doi.org/10.1080/07352680600899973

A. ter Halle, D. Lavieille, C. Richard. The effect of mixing two herbicides mesotrione and nicosulfuron on their photochemical reactivity on cuticular wax film. Chemosphere (2010) 79, 482-487 doi.org/10.1016/j.chemosphere.2010.01.003Get rights and content

S. Hamdache, M. Sleiman, P. de Sainte-Claire, F. Jaber, C. Richard. Unravelling the reactivity of bifenazate in water and on vegetables: Kinetics and byproducts. Sci. Tot. Environ. (2018) 636, 107-114 doi.org/10.1016/j.scitotenv.2018.04.219

A. Hammerbacher, T. A. Coutinho, J. Gershenzon. Roles of plant volatiles in defence against microbial pathogens and microbial exploitation of volatiles. Plant cell environ. (2019) 42, 2827-2843. doi.org/10.1111/pce13602

J. R. Hurst, J. D. McDonald, Gary B. Schuster.Lifetime of Singlet Oxygen in Solution Directly Determined by Laser Spectroscopy. J. Am. Chem. Soc. 1982, 104, 2065-2067.
doi-org.ezproxy.uca.fr/10.1021/ja00371a065

T. Katagi. Photodegradation of Pesticides on Plant and Soil Surfaces. Rev Environ Contam Toxicol (2004) 182,1-195.
doi.org/10.1007/978-1-4419-9098-3_1

J.L. Martínez Vidal, P. Plaza-Bolaños, R. Romero-González, A. Garrido Frenich. Determination of pesticide transformation products: A review of extraction and detection methods. J. Chromat. A (2009) 1216, 6767-6788
doi.org/10.1016/j.chroma.2009.08.013

G. Marussi, D. Vione. Secondary Formation of Aromatic Nitroderivatives of Environmental Concern: Photonitration Processes Triggered by the Photolysis of Nitrate and Nitrite Ions in Aqueous Solution. Molecules (2021) 26, 2550
doi.org/10.3390/molecules26092550

B. Mathon, M. Ferréol, M. Coquery, J.-M. Choubert, J.-M. Chovelon, C. Miège. Direct photodegradation of 36 organic micropollutants under simulated solar radiation: Comparison with free-water surface constructed wetland and influence of chemical structure. J. Hazard. Mat. (2021) 407, 124801
doi.org/10.1016/j.jhazmat.2020.124801

592 A. Mellouki, T. J. Wallington, J. Chen. Atmospheric Chemistry of Oxygenated Volatile
593 Organic Compounds: Impacts on Air Quality and Climate. Chem. Rev. (2015) 115, 3984–
594 4014
595 doi.org/10.1021/cr500549n
596
597 T. Mochizuki ; F. Ikeda ; A. Tani. Effect of growth temperature on monoterpene emission
598 rates of Acer palmatum. Sci. Tot. Environ. (2020) 745, 140886
599 doi.org/10.1016/j.scitotenv.2020.140886
600
601 S. Monadjemi, M. el Roz, C. Richard, A. ter Halle. Photoreduction of chlorothalonil fungicide
602 on plant leaf models. Environ. Sci. Technol. (2011) 45, 9582-9589
603 doi.org/10.1021/es202400s
604
605 S. L. Murov, I. Carmichael, G. L Hug. Handbook of Photochemistry Second Edition, Marcel
606 Dekker, NY, 1993.
607
608 R. Ossola, O. M. Jönsson, K. Moor, K. McNeill. Singlet Oxygen Quantum Yields in
609 Environmental Waters. Chem. Rev. (2021) 121, 4100-4146
610 doi.org/10.1021/acs.chemrev.0c00781
611
612 D. Palma, Y. Arbid, M. Sleiman, P. De Sainte-Claire, C. Richard. New Route to Toxic Nitro
613 and Nitroso Products upon Irradiation of Micropollutant Mixtures Containing Imidacloprid:
614 Role of NO_x and Effect of Natural Organic Matter. Environ. Sci. Technol. (2020) 54, 3325–
615 3333
616 doi.org//10.1021/acs.est.9b07304
617

618 S.O. Pehkonen, Q. Zhang. The Degradation of Organophosphorus Pesticides in Natural
619 Waters: A Critical Review. Crit Rev Environ Sci Technol. (2002) 32, 17-72.
620 doi.org/10.1080/10643380290813444
621
622 J. Petrović, D. Stojković, M. Soković. Chapter Eight - Terpene core in selected aromatic and
623 edible plants: Natural health improving agents. Adv. Food Nutr. Res. (2019) 90, 423-451
624 doi.org/10.1016/bs.afnr.2019.02.009
625
626 J. Porras, J ; J. Fernandez, R. A. Torres-Palma, C. Richard. Humic substances enhance
627 chlorothalonil phototransformation via photoreduction and energy transfer. Environ. Sci.
628 Technol. (2014) 48, 2218-2225.
629 doi.org/10.1021/es404240x
630
631 S. C. Remke, U. Gunten, S. Canonica.Enhanced transformation of aquatic organic compounds
632 by long-lived photooxidants (LLPO) produced from dissolved organic matter. Water Res.
633 (2021) 9, 116707
634 doi.org/10.1016/j.watres.2020.116707
635
636 C. K. Remucal. The role of indirect photochemical degradation in the environmental fate of
637 pesticides: a review. Environ. Sci.: Processes Impacts (2014) 16, 628-653
638 doi.org/10.1039/C3EM00549F
639
640 M. A. J. Rodgers, P. T. Snowden. Lifetime of ($^1O_2$) in Liquid Water As Determined by Time-
641 Resolved Infrared Luminescence Measurements. J. Am. Chem. Soc. 1982, 104, 5541-5543.
642 doi-org.ezproxy.uca.fr/10.1021/ja00384a070

B. Salehi, A. Prakash Mishra, I. Shukla, M. Sharifi- Rad, M. del Mar Contreras, A. Segura- Carretero, H. Fathi, N. Nasri Nasrabadi. Thymol, thyme, and other plant sources: Health and potential uses. Phytoter Res (2018) 32, 1688-1706
doi.org/10.1002/ptr.6109

K. Skalska, J.S. Miller, S. Ledakowicz. Trends in NOx abatement : a review. Sci. Tot. Environ. (2010) 408, 3976-3989.
doi.org/10.1016/j.scitotenv.2010.06.001

R. M. de Souza, D. Seibert, H.B. Quesada, F. J. Bassetti, M.R. Fagundes-Klen, R. Bergamasco. Occurrence, impacts and general aspects of pesticides in surface water: A review. Process Saf Environ Prot (2020) 135, 22-37
doi.org/10.1016/j.psep.2019.12.035

S. Venu, D. B. Naik, S. K. Sarkar, U. K. Aravind, A. Nijamudheen, C. T. Aravindakumar. Oxidation Reactions of Thymol: A Pulse Radiolysis and Theoretical Study. J. Phys. Chem. A (2013) 117, 291–299
doi.org/10.1021/jp3082358

D. Vione, C. Minero, F. Housari, S. Chiron. Photoinduced transformation processes of 2,4-dichlorophenol and 2,6-dichlorophenol on nitrate irradiation. Chemosphere (2007) 69, 1548–1554
doi.org/10.1016/j.chemosphere.2007.05.071

668 E.D. Wannaz, J.A. Zygadlo , M.L. Pignata. Air pollutants effect on monoterpenes
669 composition and foliar chemical parameters in Schinus areira L. Sci. Tot. Environ. (2003)
670 305, 177-193
671 doi.org/10.1016/S0048-9697(02)00466-7
672
673 F. Wilkinson, J.G. Brummer. Rate constants for the decay and reactions of the lowest
674 electronically excites singlet state of molecular oxygen in solution. J. Phys. Chem. Ref. Data
675 1981, 10, 809-999.
676 doi.org/10.1063/1.555965
677
678 T. Zeng, W. A. Arnold. Pesticide Photolysis in Prairie Potholes: Probing Photosensitized
679 Processes. Environ. Sci. Technol. (2013) 47, 6735–6745
680 doi.org/10.1021/es3030808
681
682
683